Supporting Information

Interplay between Crystal's Shape and Spatiotemporal Dynamics in the Spin Transition material.

Houcem Fourati[a,b], Eric Milin[c], Ahmed Slimani[d], Guillaume Chastanet[e], Younes Abid [b], Smail Triki[c] and Kamel Boukheddaden[a*]

[a]*Groupe d'Etudes de la Matière Condensée, Université de Versailles, Université Paris-Saclay, CNRS UMR CNRS 8635, 45 Avenue des Etats Unis 78035 Versailles*

[b]*Laboratoire de Physique Appliquée, Faculté des Sciences de Sfax, Université de Sfax, Route de Soukra km 3.5, 3000, Sfax, Tunisia*

[c]*Laboratoire de Chimie, Electrochimie Moléculaires, Chimie Analytique, UMR CNRS 6521- Université de Brest, 6 Av. V. Le Gorgeu, CS 93837, 29238 Brest, France*

[d]*Laboratoire des Matériaux Multifonctionnels et Applications, Département de physique, Faculté des Sciences de Sfax, Université de Sfax, Route de la Soukra km 3.5 – B.P. n° 1171 – 3000, Sfax, Tunisia*

[e]*Institut de Chimie de la Matière Condensée de Bordeaux, Université de Bordeaux, 87 Av. Doc. A. Schweitzer, F-33608 Pessac, France*

**corresponding author: kamel.boukheddaden@uvsq.fr*

1 - Synthesis and general characterizations.

General characterizations. 2-aminopyridine, diformylhydrazine, potassium tetracyanopalladate ($K[Pd(CN)_4].xH_2O$) and iron (II) perchlorate were purchased respectively from Alfa Aesar and Sigma-Aldrich, and used without further purification. Solvents were used and purified by standard procedures. Elemental analyses were performed by the "Service Central d'Analyses du CNRS", Gif-sur-Yvette, France. Infrared spectra were recorded in the range 4000-400 cm^{-1} on a FT-IR Brucker ATR Vertex 70 Spectrometer. Single crystal X-ray studies were performed at 296 K using a Xcalibur 2 κ-CCD diffractometer using Mo Kα

radiation (λ = 0.71073 Å). The crystal structure was solved by direct methods with the SHELXS program and refined on F^2 by weighted full matrix least-squares methods using the SHELXL program.[1] All non-hydrogen atoms were refined anisotropically, hydrogen atoms were located in difference Fourier maps and treated using a riding model. Crystallographic data and refinement details are provided in Table S1. NMR spectra were recorded on a Bruker DRX 300MHz. DSC measurements were performed on a DSC-1/LN2 Mettler Toledo calorimeter setting the heat flow scan rate at s = 0.4 K•min^{-1}.

Synthesis of 4-(2-pyridyl)-1,2,4, 4H-triazole. The 4-(2-pyridyl)-1,2,4,4H-triazole (2-pytrz) was prepared using the procedure described in reference 2 (Yield: 1.21 g, 36 %). m.p. 169 °C. IR data (ν/cm^{-1}): 3220(w), 3124(w), 2907(w), 2134(m), 2123(m), 1615(m), 1593(m), 1518(m), 1502(w), 1481(s), 1463(w), 1463 (m), 1441(m), 1367(m), 1338(m), 1264(m), 1238(m), 1160(m), 1112(m), 1095(m), 1053(m), 1012(m), 991(m), 945(w), 896(w), 877(w), 838(w), 787(s), 737(m), 712(m), 632 (m), 621(m), 520(m), 464(m). NMR ^{1}H (300 MHz, D_2O): 7.35-7.39 (t, 1H); 7.68-7.71 (d, 1H); 7.92-7.96 (t,1H); 8.45-8.47 (d,1H); 9.17 (s, 2H (trz)). NMR ^{13}C (75 MHz, D_2O): 118.1(C-H(pyr)); 127.3(C-H(pyr)); 143.6(C-H(pyr)); 144.2(C(α-Npyr)); 151.8(C-H(α-Npyr); 165.2(C-H (trz)).

Synthesis of [Fe(2-pytrz)$_2${Pd(CN)$_4$}].3H$_2$O (1). An aqueous solution (10 mL) containing the 4-(2-pyridyl)-1,2,4,4*H*-triazole (146.0 mg, 1.0 mmol),[2] iron (II) perchlorate (127.5 mg, 0.5 mmol) was left standing overnight. To the resulting light yellow solution, was added $K_2[Pd(CN)_4].xH_2O$ (144.5 mg, 0.5 mmol) and the mixture was stirred at room temperature. The resulting white precipitate was filtered off and dried (yield 65 %, 199.3 mg). Anal. Calcd for $C_{18}H_{18}FeN_{12}O_3Pd$: C, 35.2; H, 2.9; N, 27.4 %. Found: C, 34.9; H, 3.0; N, 27.0 % (see Figure S2 for IR data). Single-crystals of **1** were prepared by slow diffusion, in a fine glass tube (3.0 mm diameter) of two aqueous solutions: the first solution was obtained by dissolving $K_2[Pd(CN)_4].xH_2O$ (28.9 mg, 0.1mmol) in 10 mL. The second solution was prepared by dissolving $Fe(ClO_4)_2.xH_2O$ (25.5 mg, 0.1 mmol) in a solution (10 mL) of 4-(2-pyridyl)-1,2,4,4H-triazole (29.2 mg, 0.2 mmol). After standing overnight, a light yellow coloration was appeared. 2 mL of the $K_2[Pd(CN)_4].xH_2O$ solution was placed in the fine glass tube and 2 mL of the yellow solution was added carefully. After three days, colorless small fine square crystals of **1** were formed by slow diffusion.

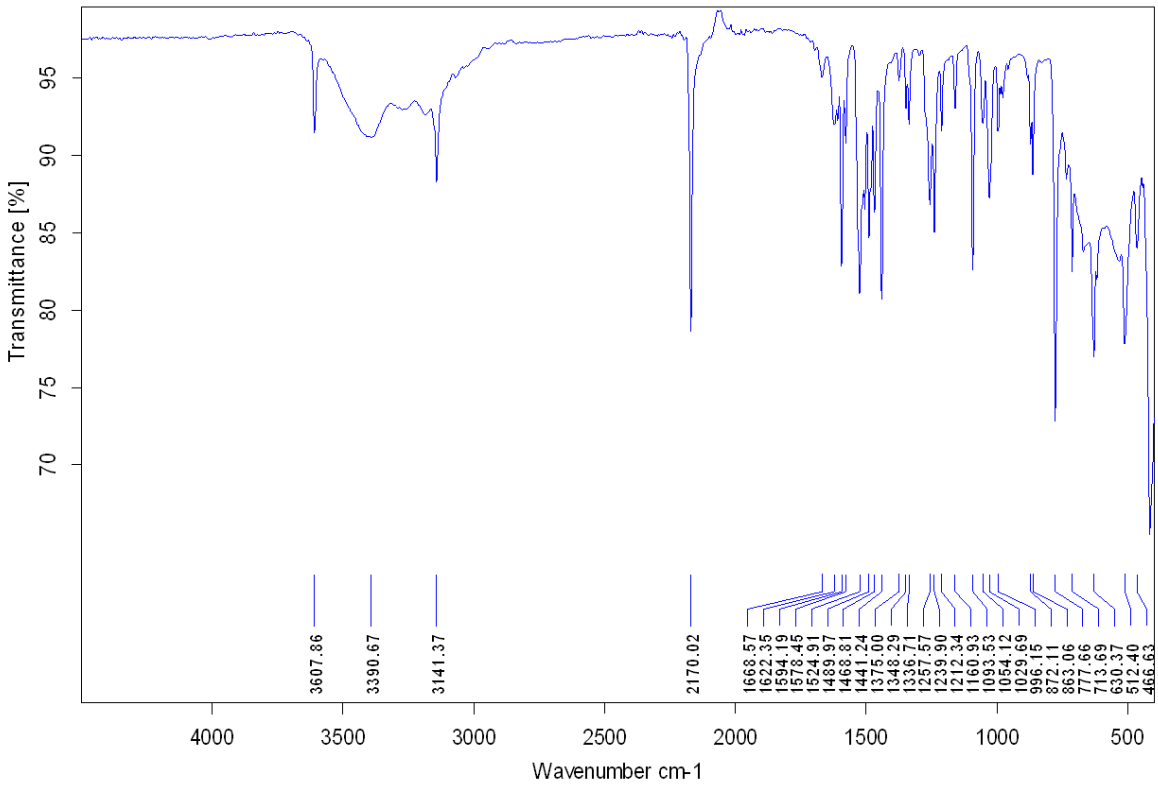

Figure S1. IR spectrum of the single crystals of $[Fe(2\text{-pytrz})_2\{Pd(CN)_4\}].3H_2O$ (**1**): IR data (ν/cm^{-1}): 3608(w), 3391(br), 3141(m), 2170(s), 1622(s), 1594(s), 1525(s), 1490(m), 1469(m), 1441(m), 1375(w), 1348(w), 1337(w), 1258(m), 1240(m), 1212(w), 1161(w), 1094(w), 1054(s), 1030(w), 996(w), 872(w), 863(m), 778(s), 714(w), 630(s), 512(m), 467(m).

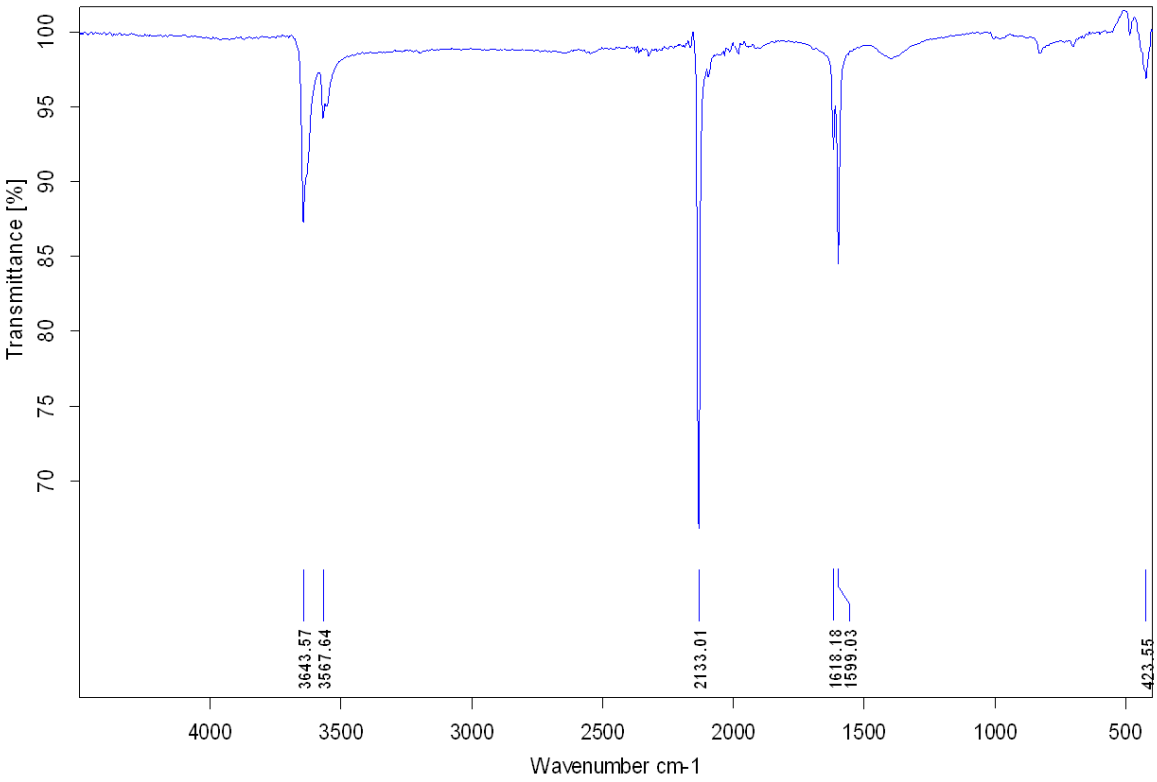

Figure S2. IR spectrum of $K_2[Pd(CN)_4]\ xH_2O$.

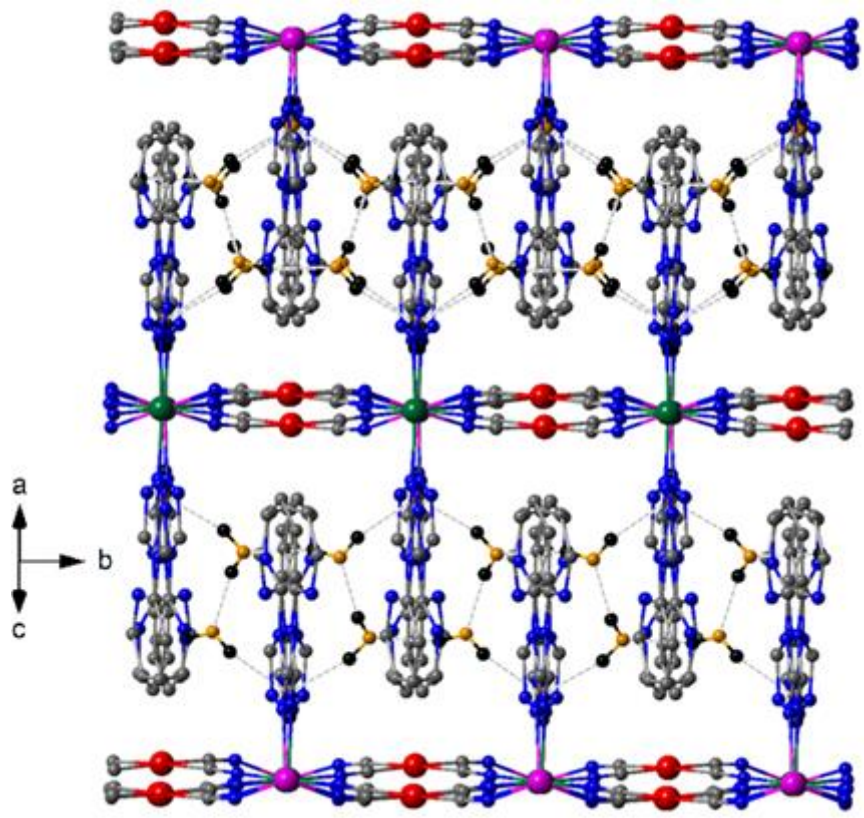

Figure S3. 3-D View of the crystal packing of 1 at 298 K. Dashed lines show the hydrogen-bonding network.

2 – Structural characterization

Table S1. Crystallographic data for compound **1**

T / K	298
Color	colorless
[a]Chemical formula	$C_{18}H_{18}FeN_{12}O_3Pd$
Formula weight	612.69
Crystal system	Monoclinic
Space group	C2/c
a/Å	25.222(3)
b/Å	7.4054(7)
c/Å	27.298(3)
β/°	111.464(13)
Volume/Å^3	4745.2(10)
Z	8
ρ_{calc} g/cm^3	1.715
[b]Final R_1 / wR_2	0.0409 / 0.0762
[c]GOF on F^2	0.926

[a]There is one chemical formula in the asymmetric unit.[b] $R_1 = \sum|Fo - FC|/Fo)$ $[I \geq 2\sigma\ (I)]$ and $wR_2 = [\sum((\omega(Fo^2 - Fc^2))^2/\omega(Fo^2))^2]^{1/2}$ [all data].[c] $G.O.F = \left[(\sum\left(\omega(Fo^2 - Fc^2)\right)^2/(Nobs - Nvar)\right]^{1/2}$

3. List of deposited movie files:

Movie SM1: Visualization of the spatiotemporal transformation on cooling of the rectangularly-shaped [Fe(2-pytrz)$_2${Pd(CN)$_4$}].3H$_2$O single crystal. The cooling rate is $r = 0.2\ K.min^{-1}$ and the shinning intensity of the optical microscope lamp, $I = I_{min} = 0.3\ mWcm^{-2}$.

Movie SM2: Visualization of the spatiotemporal transformation on heating of the rectangularly-shaped single crystal. The heating rate is $r = 0.2\ K.min^{-1}$ and the shinning intensity of the optical microscope lamp, $I = 0.3\ mWcm^{-2}$.

Movie SM3: Visualization of the spatiotemporal transformation on cooling of the triangular [Fe(2-pytrz)$_2${Pd(CN)$_4$}].3H$_2$O single crystal. The cooling rate is $r = 0.2\ K.min^{-1}$ and the shinning intensity of the optical microscope lamp, $I = 0.3\ mWcm^{-2}$.

Movie SM4: Visualization of the spatiotemporal transformation on heating of the triangular single crystal. The heating rate is $r = 0.2\ K.min^{-1}$ and the shinning intensity of the optical microscope lamp, $I\ = 0.3\ mWcm^{-2}$.

Movie SM5: Simulated spatiotemporal behavior of the HS fraction on cooling of the rectangularly-shaped along the theoretical thermal hysteresis of Fig. 9 of the main manuscript. The initial temperature was 112 K (smaller than the equilibrium temperature) and the used scan rate $r = 0.2\ K.s^{-1}$ where time is in arbitrary unit. The spatiotemporal behavior of the front is very similar to that of the experimental movie (S1).

Movie SM6: Simulated spatiotemporal behavior of the HS fraction on heating of the rectangularly-shaped along the theoretical thermal hysteresis of Fig. 9 of the main manuscript. The initial temperature was 114 K (bigger than the equilibrium temperature) and the used scan rate $r = 0.2\ K.s^{-1}$ where time is in arbitrary unit. The spatiotemporal behavior of the front is very similar to that of the experimental movie (S2).

Movie SM7: Simulated spatiotemporal behavior of the HS fraction on cooling of the triangular along the theoretical thermal hysteresis of Fig. 9 of the main manuscript. The initial temperature was 112 K (smaller than the equilibrium temperature) and the used scan rate $r = 0.2\ K.s^{-1}$ where time is in arbitrary unit. The spatiotemporal behavior of the front is very similar to that of the experimental movie (S3).

Movie SM8: Simulated spatiotemporal behavior of the HS fraction on heating of the triangular along the theoretical thermal hysteresis of Fig. 9 of the main manuscript. The initial temperature was 114 K (bigger than the equilibrium temperature) and the used scan rate $r = 0.2\ K.s^{-1}$ where time is in arbitrary unit. The spatiotemporal behavior of the front is very similar to that of the experimental movie (S4).

Movie SM9: Simulated spatiotemporal behavior of the HS fraction on cooling of the rectangular crystal along the theoretical thermal hysteresis of Fig. 9 of the main manuscript. The initial temperature was 112 K (smaller than the equilibrium temperature) and the used scan rate was $r = 0.2\ K.u^{-1}$ where time is in arbitrary unit. In this case the considered diffusion parameter was isotropic.

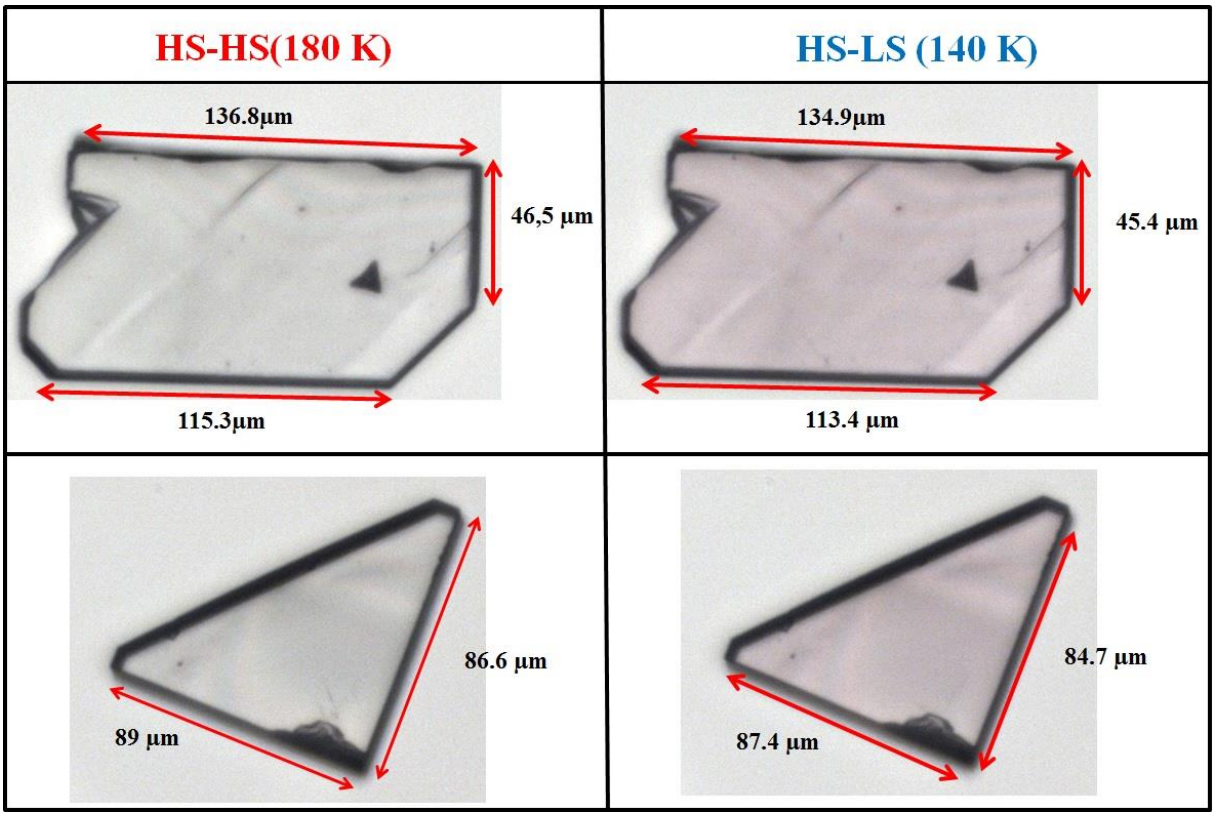

Figure S4: OM images of **R** and **T** single crystals giving their sizes in the high and low-temperature phases corresponding to the HS and intermediate HS-LS states, respectively.

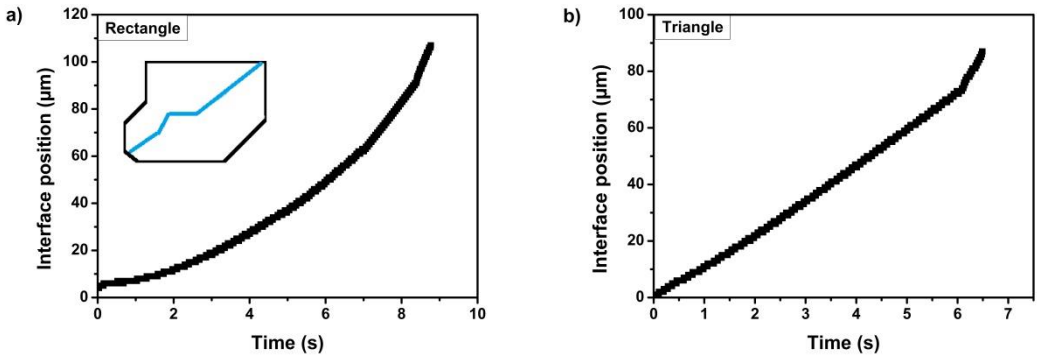

Figure S5: Theoretical interface position as a function of time during heating process of the simulated rectangle (a) and triangle (b) lattices.

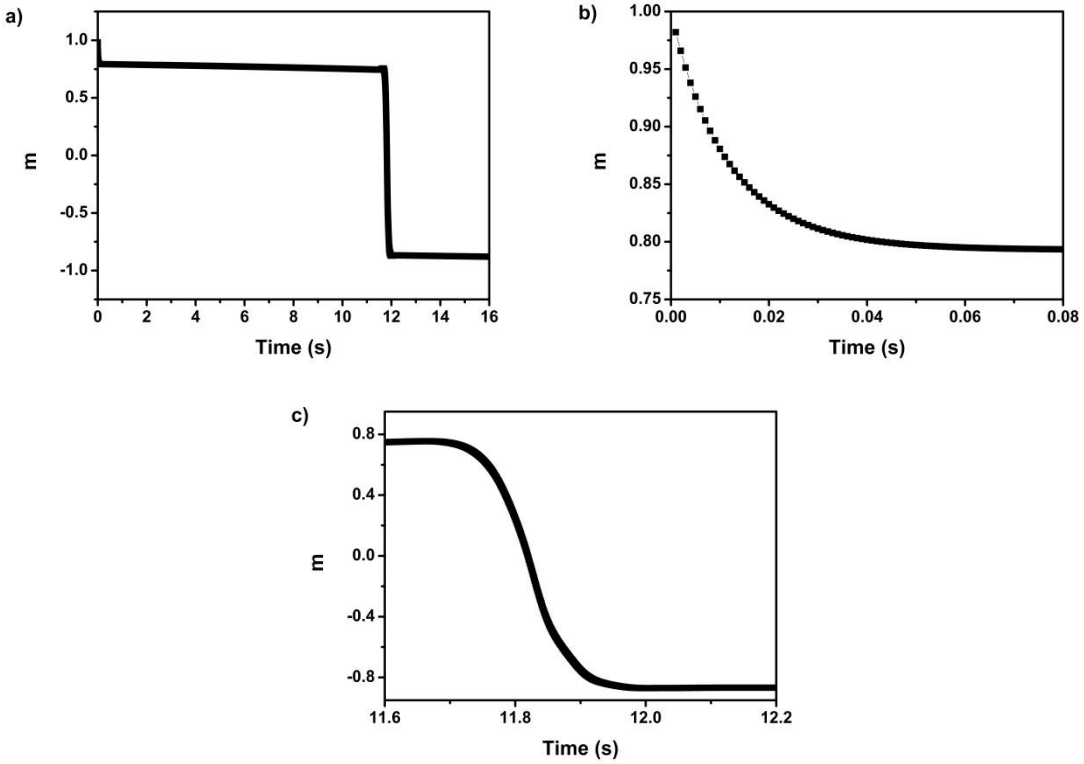

Figure S6 : Local kinetic curve, temporal evolution of the magnetization at a given position. a) the overall the transition, b) the first regime with an exponential decrease of the fictitious magnetization, c) the transition to the new state (LS) with a sigmoidal behavior.

References:

[1] Sheldrick, G. M., *Acta Cryst*. **2008**, *A64*, 112.

[2] Wiley, R.H.; Hart, A. J. *J. Org. Chem.* **1953**, *18*, 1368-1371